RESEARCH ARTICLE | JULY 15 1987

Oriented growth of niobium and molybdenum on GaAs crystals

M. Eizenberg; Armin Segmüller; M. Heiblum; D. A. Smith

J. Appl. Phys. 62, 466–473 (1987)
https://doi.org/10.1063/1.339768

Oriented growth of niobium and molybdenum on GaAs crystals

M. Eizenberg,[a] Armin Segmüller, M. Heiblum, and D. A. Smith
IBM Thomas J. Watson Research Center, P.O. Box 218, Yorktown Heights, New York 10598

(Received 15 January 1987; accepted for publication 12 March 1987)

Thin layers of Mo and Nb, 100–400 Å thick, were deposited onto clean (100) and $(\bar{1}\bar{1}\bar{1})$GaAs substrates under ultrahigh vacuum conditions in a molecular-beam epitaxy system, at slow rates and at relatively low temperatures. The microstructure of the films and the orientation relationship with the substrates were determined by *in situ* reflection high-energy electron diffraction, by transmission electron microscopy, and by grazing-incidence x-ray diffraction. In spite of the large lattice mismatch to GaAs (11% for Mo and 17% for Nb) and the low deposition temperatures(<400 °C), oriented deposits were obtained on both substrates for both metals. Although both metals are body-centered cubic with similar lattice parameters, and are both of similar chemical behavior, they grow differently on GaAs. Molybdenum grows epitaxially in the (111) orientation on both (100) and $(\bar{1}\bar{1}\bar{1})$GaAs substrates, whereas niobium grows with the (100) orientation on (100)GaAs, and with no simple orientation on $(\bar{1}\bar{1}\bar{1})$GaAs. In both cases, the orientational spread (deduced from the diffraction patterns) is smallest when the lattice planes parallel to the interface have the same symmetry in film and substrate.

I. INTRODUCTION

There is a growing interest in the structure and properties of interfaces between metals and semiconductors because of their importance in electronic and optoelectronic devices.[1] These properties strongly depend on the cleanliness of the environment before and during deposition of the materials. Ideal samples for study can be prepared in a molecular-beam epitaxy (MBE) system which enables the growth of clean, high-quality, single-crystal materials. The development of the structure and the orientation of substrate and deposit can be followed in real time by using the built-in reflection high-energy electron diffraction (RHEED) instrumentation.

There is particular interest in the epitaxial growth of metals on GaAs single-crystal substrates because of the potential use of such structures in some devices, e.g., the metal-base transistor.[2] Metals which have a good lattice match with GaAs, and indeed grow epitaxially on it, are the face-centered cubic (fcc) metals, aluminum[3] and gold.[4] However, their high reactivity with GaAs at relatively low temperatures may exclude them from being implemented in actual devices. The body-centered cubic (bcc) refractory metals, which are more inert on GaAs, are better candidates for this purpose. Unfortunately, the low-index lattice planes of these bcc metals show a large misfit ($>10\%$) with the low-index planes of GaAs. The possibility of epitaxy in such cases is an interesting issue. Two nonrefractory bcc metals with small misfit have recently been grown epitaxially on GaAs: Iron on a (100) (Ref. 5) and a (110) (Ref. 6) substrate ($\sim 1.4\%$ misfit), and metastable bcc cobalt on a (110) substrate (~ 0 misfit).[7]

Epitaxial growth of two refractory metals, tungsten and molybdenum, that have a large lattice mismatch with GaAs, has recently been tried[8] on the (100) substrate plane in ultrahigh vacuum at substrate temperatures $T_s < 500$ °C. It was found that tungsten could be grown in this temperature range only as a randomly oriented polycrystalline film. More encouraging results were obtained for Mo, where in the temperature range $200 < T_s < 450$ °C, very small crystallites grew epitaxially with their (111) plane parallel to the (100)GaAs substrate.[8,9] These results motivated us to study further the possibilities of epitaxial growth of two refractory bcc metals, molybdenum and niobium, on two differently oriented substrates of GaAs, (100) and $(\bar{1}\bar{1}\bar{1})$. Preliminary results for Nb on (100)GaAs have been published elsewhere.[10]

II. EXPERIMENTAL PROCEDURES

The depositions were carried out in a Riber 1000-1 MBE system, with a residual gas pressure during deposition of $\sim 5\times 10^{-10}$ Torr. First, a GaAs epilayer, ~ 1 μm thick and doped with Si $\sim 1\times 10^{18}$ cm^{-3}, was grown on an n^+-(100)GaAs substrate at a temperature of 600 °C. Then, the sample temperature was gradually reduced to the desired substrate temperature for the metal growth T_s. When the As background pressure reached $\sim 10^{-11}$ Torr after ~ 3 h, a thin metal layer, with a thickness ranging from 100 to 400 Å, was deposited by a 5-kW electrostatic electron-gun evaporator[11] especially designed to minimize the escape of stray electrons that can cause impurity desorption from the walls. In order to minimize background impurities, the deposition rate, determined by the extent of heating of the electron-gun evaporator, was kept low at a rate of 1–3 Å/min. Several different substrate temperatures in the range between 40 and 400 °C were used for different growth runs, and this variation was found to affect the orientation of the deposit, as will be discussed later.

The characterization of the films was focused mainly on their microstructure and their orientation relationship with

[a] Permanent address: Dept. of Materials Engineering and the Solid State Institute, Technion—Israel Institute of Technology, Haifa 32000, Israel.

 0021-8979/87/140466-08$02.40

the substrate. *In situ* analysis was performed by RHEED, which monitors the crystallography of the top few atomic layers during growth. After deposition, the samples were analyzed outside the MBE system by transmission electron microscopy (TEM), and by grazing-incidence x-ray diffraction (GID), a technique recently described by Marra, Eisenberger, and Cho.[12] In the latter method, a monochromated and slightly focused x-ray beam is incident on the horizontal sample surface at an angle close to and slightly above the critical angle for total reflection ($\lesssim 0.5°$). In a very shallow surface layer, $\lesssim 1000$ Å thick, diffraction can take place at lattice planes (hkl) perpendicular to the surface with considerable intensity. The diffracted beam exits the sample surface under an equally shallow angle, inclined at twice the Bragg angle θ_{hkl} to the incident beam. To characterize crystallite size and strain, both parallel to the interface, 2θ-θ or radial scans were performed. Lattice parameters and macroscopic strains are determined from the Bragg angle, and the crystallite size is estimated from the full width at half maximum (FWHM) of the diffraction lines according to Scherrer's equation.[13] To establish the substrate/deposit orientation relationship, a strong reflection was sought for both the substrate and the film. Then, the detector for the diffracted x-rays was fixed at $2\theta_{hkl}$ of the film reflection, and the sample was rotated around the surface normal in a so-called ω scan.[9] With GID, films can be characterized that are too thin for conventional Bragg diffraction on a powder diffractometer. It is noted that with GID the crystallinity is studied parallel to the interface, whereas with conventional x-ray diffraction crystal properties are characterized along a direction parallel to the interface normal or inclined to it by an angle much less than 90°. GID allows nondestructive characterization of the bilayers, whereas for TEM characterization, the substrates had to be thinned from the back by chemical etching.

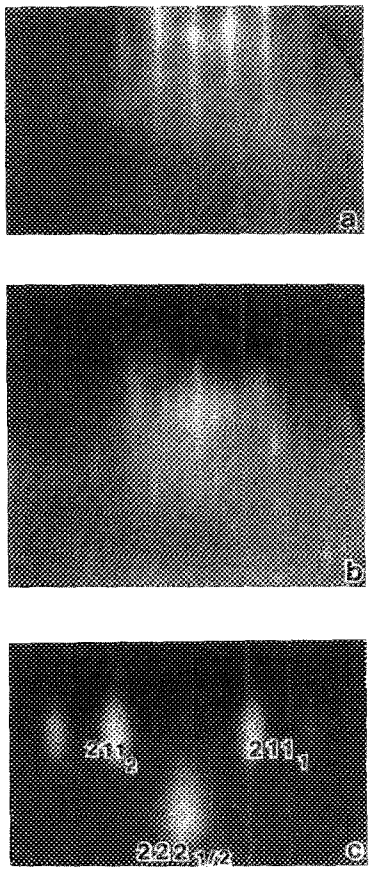

FIG. 1. RHEED pattern showing the 2×2 and $\sqrt{19}\times\sqrt{19}$ reconstructions of $(\bar{1}\bar{1}\bar{1})$GaAs [(a) and (b), respectively], and (c) formation of epitaxial (111) Mo film. Beam direction $[01\bar{1}]$GaAs azimuth.

III. RESULTS

In situ observation by RHEED of the (100) oriented epilayer of GaAs, prior to the metal deposition, showed the surface to be (4×6) reconstructed in most cases; for a few samples, the As-stabilized $c(2\times8)$ reconstruction was observed. For the $(\bar{1}\bar{1}\bar{1})$ oriented substrates, two types of reconstructions could be obtained depending on the growth parameters: the As-rich (2×2) and the Ga-stabilized $(\sqrt{19}\times\sqrt{19})-23.5°$, as shown in Figs. 1(a) and 1(b), respectively. It was found that the properties of the metal deposits were independent of the GaAs reconstruction, since the reconstructions disappeared as soon as metal deposition commenced, and only the bulk pattern of GaAs was observed up to a deposit thickness of ~ 5 Å, when it also disappeared. No diffraction spots at all were visible until the metal (either Mo or Nb) thickness was about 30 Å, whereupon a RHEED pattern characteristic of crystalline metal deposit was observed (in the case of Nb only for $T_s \lesssim 270$ °C). This result, reported also in Ref. 8, indicates that crystallization of the deposit occurred only after this critical thickness had been reached.[14]

The RHEED pattern observed for Mo consisted of quite sharp and elongated spots suggesting that large portions of the deposit were aligned, epitaxially oriented with respect to the substrate. The sharpness of the pattern was improved as T_s was increased (up to 375 °C). A typical pattern for Mo on $(\bar{1}\bar{1}\bar{1})$GaAs, with the incident beam along the substrate $[0\bar{1}]$ direction, is presented in Fig. 1(c). This pattern can be interpreted as belonging to two domains of Mo with the epitaxial relationship $(111)\text{Mo}\|(\bar{1}\bar{1}\bar{1})\text{GaAs}$ with $[01\bar{1}]\text{Mo}\|[01\bar{1}]\text{GaAs}$ and $[0\bar{1}1]\text{Mo}\|[01\bar{1}]\text{GaAs}$ which was confirmed by TEM and GID. For Mo deposited on (100)GaAs, we reported earlier[8,9] the epitaxial relationship $(111)\text{Mo}\|(100)\text{GaAs}$ with $[0\bar{1}1]\text{Mo}\|[011]\text{GaAs}$ and $[0\bar{1}1]\text{Mo}\|[0\bar{1}1]\text{GaAs}$.

The growth of Nb on GaAs, as monitored *in situ* by RHEED and later verified by TEM and GID, differs from that of Mo. The RHEED pattern observed in the substrate temperature range from 100–270 °C consisted of broad spots from Nb suggesting that the deposit consisted of small, possibly strained crystals, and was continuous. A typical pattern for Nb on (100)GaAs with the incident beam along the substrate [011] direction is presented in Fig. 2. This pattern can be interpreted as belonging to the (100) Nb surface along the [001] direction, indicating an epitaxial relationship $(100)\text{Nb}\|(100)\text{GaAs}$ and $[001]\text{Nb}\|[011]\text{GaAs}$. For $T_s < 100$ °C only blurred rings were observed by RHEED, indicating randomly oriented fine-grained polycrystalline

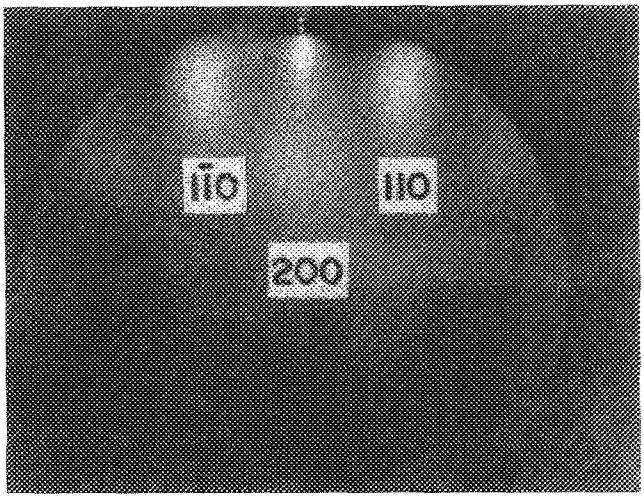

FIG. 2. RHEED pattern showing formation of aligned (100)Nb film. Beam direction: [001]Nb|| [011]GaAs.

growth, while for 270 °C $< T_s <$ 400 °C, no pattern could be observed at all after the disappearance of the GaAs substrate pattern. Niobium films were also deposited on the $(\bar{1}\bar{1}\bar{1})$ plane of GaAs in the same temperature range. Monitoring by RHEED and subsequent study by TEM established the orientation relationship (100)Nb||$(\bar{1}\bar{1}\bar{1})$GaAs, but without a well-defined azimuthal orientation.

More information about the microstructure of the deposit and its relationship to the substrate was obtained by TEM. Figures 3(a)–3(d) show the transmission electron diffraction patterns (beam perpendicular to the surface) for Mo on (100) and $(\bar{1}\bar{1}\bar{1})$GaAs and Nb on (100) and $(\bar{1}\bar{1}\bar{1})$GaAs, respectively. These are the optimum results for each case with $T_s = 375$ and 170 °C for Mo and Nb, respectively. In addition to the substrate diffraction spots, elongated spots corresponding to the deposit can be observed in all patterns. The six- and four-fold symmetries of the Mo and Nb patterns, respectively, on both substrates studied, and their relationship with the substrate patterns, confirm the orientation relationship already established *in situ* by RHEED.

The texture of Nb on $(\bar{1}\bar{1}\bar{1})$GaAs [Fig. 3(d)] is difficult to explain. The (110)Nb diffraction ring, just inside the six somewhat diffuse (220)GaAs diffraction spots, is continuous with eight arc-shaped areas of higher intensity. However, these arcs arranged in an almost fourfold symmetry pattern do not have any clear orientational relationship to the substrate with its threefold symmetry. The presence of (110), (200), and (310)Nb diffraction spots (or rings), and the absence of (211)Nb diffraction spots, together with the findings by *in situ* RHEED, indicate that this Nb film has a restricted (100) fiber texture. The occurrence of continuous

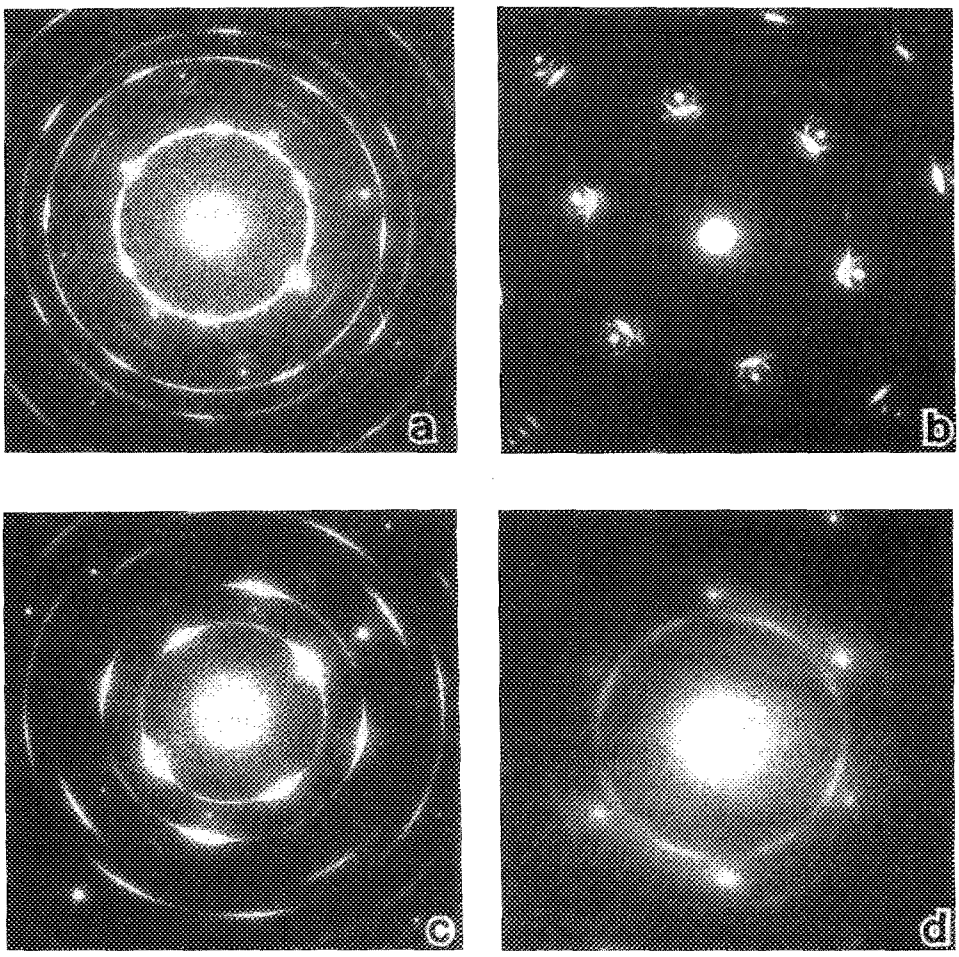

FIG. 3. Transmission electron diffraction patterns for (a) Mo deposited on (100)GaAs; (b) Mo deposited on $(\bar{1}\bar{1}\bar{1})$GaAs; (c) Nb deposited on (100)GaAs; (d) Nb deposited on $(\bar{1}\bar{1}\bar{1})$GaAs.

rings in the Nb diffraction patterns and sometimes also for Mo on (100)GaAs, in addition to the strong elongated spots, indicates the presence of some randomly oriented crystallites. The elongated shape of the deposit diffraction spots suggests that the crystallites aligned with the substrate are small and have some mosaic spread about the exact epitaxial orientation. We note the arcing to be much smaller for Mo than for Nb. The orientational spread of Mo films is smaller on the $(\bar{1}\bar{1}\bar{1})$ than on the (100)GaAs substrate, while for Nb films the opposite is observed.

For the four cases studied (corresponding to Fig. 3), (011) dark-field TEM images of the aligned crystallites are given in Figs. 4(a)–4(d). They reveal areas free of high-angle grain boundaries that extend for several hundred nanometers. From these figures the proportion of epitaxially aligned crystallites is probably underestimated, since some of the aligned crystallites may not be imaged because of bending during the specimen preparation and observation.

The dependence of the "quality" of the epitaxy on the substrate temperature during deposition, as deduced from the TEM diffraction patterns, was different for Mo than for Nb. In the former case, as T_s was increased up to 375 °C, the spots became sharper and the intensity from the nonaligned deposit decreased. Higher temperatures were not investigated to avoid chemical reaction between Mo and GaAs that takes place at $T_s \sim 500$ °C.[8] We note, however, that postdeposition annealing inside the TEM to a temperature as high as 650 °C has not produced any detectable compounds. In the case of Nb, however, a gradual decrease in the intensity of the maxima in the diffraction pattern was observed as the substrate temperature during growth was either decreased or increased from the optimum $T_s = 170$ °C, confirming the results obtained *in situ* by RHEED. When this optimal film was heated inside the TEM to ~440 °C, extra rings appeared, as shown in Fig. 5, that could be attributed to the formation of the compound NbAs.[15] The azimuthal variation in intensity shows that the compound grew in a preferred orientation.

X-ray diffraction patterns of the Mo and Nb films were recorded by GID in radial scans and ω scans. The ω-scan data of the (011) reflection of Mo and Nb deposited on (100) and $(\bar{1}\bar{1}\bar{1})$GaAs are shown in Figs. 6(a)–6(d). In Fig. 6(a), Mo on (100)GaAs, the well-defined peaks of large intensity, are attributed to two domains, denoted A and B, with the epitaxial relationship (111)Mo‖(100)GaAs. In the interface, the azimuthal orientation for domains A and B is given by $[01\bar{1}]$Mo‖[011]GaAs and $[01\bar{1}]$Mo‖$[01\bar{1}]$GaAs. The weak intensity between some of

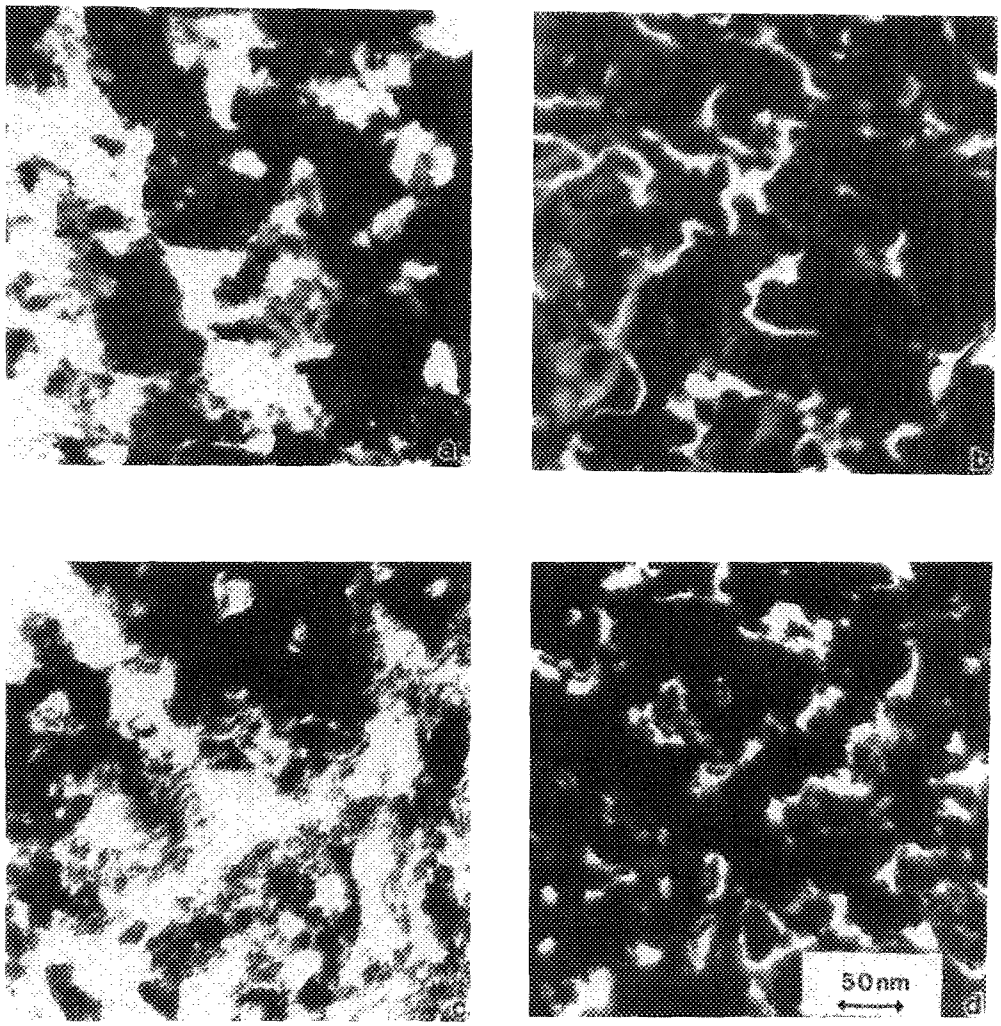

FIG. 4. (011) dark-field TEM images for (a) Mo deposited on (100)GaAs; (b) Mo deposited on $(\bar{1}\bar{1}\bar{1})$GaAs; (c) Nb deposited on (100)GaAs; (d) Nb deposited on $(\bar{1}\bar{1}\bar{1})$GaAs.

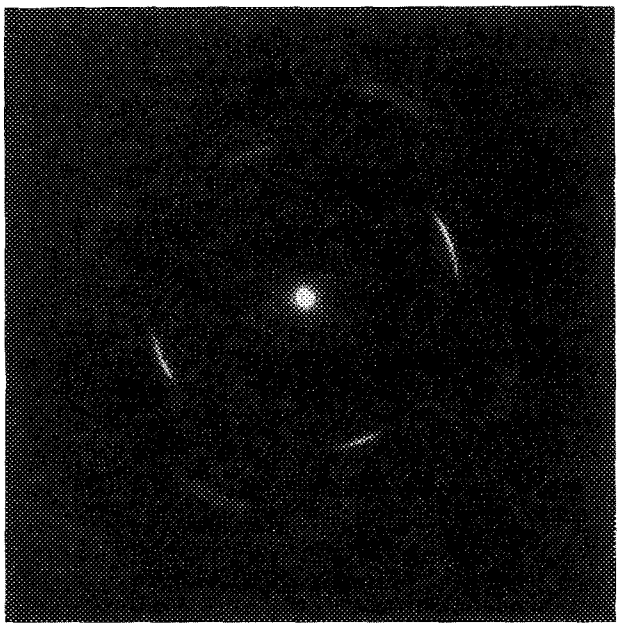

FIG. 5. Transmission electron diffraction pattern of Nb film, prepared at $T_s = 170$ °C and subsequently annealed at 440 °C for a few minutes, resulting in the formation of aligned NbAs.

the A and B peaks can be attributed to a domain C with the epitaxial relationship (100)Mo‖(100)GaAs and [011]Mo‖[010]GaAs. Domain C comprises only a small fraction of the film and it has not been detected by the other methods. From the FWHM of the A and B peaks, an orientational spread of $\pm 5.5°$ of the A and B domains can be deduced. The (011) ω-scan data for Mo on $(\bar{1}\bar{1}\bar{1})$GaAs [Fig. 6(b)], show a few well-defined peaks, with 60° spacing between them, confirming the epitaxial relationship (111)Mo‖$(\bar{1}\bar{1}\bar{1})$GaAs with $[01\bar{1}]$Mo‖$[01\bar{1}]$GaAs. The orientational spread of $\pm 1.2°$ is much smaller than that of Mo on (100)GaAs. We note that film domains differing in orientation by a rotation of 60° around the [111]Mo cannot be distinguished by GID ω scans. The (011) ω-scan data for Nb on (100)GaAs [Fig. 6(c)], show two broad peaks with 90° spacing between them, confirming the epitaxial relationship (100) Nb ‖ (100) GaAs with [011]Nb‖[001]GaAs. The orientational spread of $\pm 5.5°$ is much larger than that of Mo on $(\bar{1}\bar{1}\bar{1})$GaAs. The (011) ω-scan data for Nb on $(\bar{1}\bar{1}\bar{1})$GaAs [Fig. 6(d)], show no distinct epitaxial features. The (002) ω-scan data has a similar appearance. These results are compatible with a (100) fiber texture indicated by the RHEED study of this sample. However, the orientation distribution around the fiber axis is not completely random, as evidenced by transmission electron diffraction and GID. Therefore, this texture may be called a restricted fiber texture. From the FWHM observed in radial scans, the grain size parallel to the interface has been estimated to be ~130, 190, 180, and 130 Å for the samples represented in Figs. 6(a)–6(d), respectively. From the Bragg angle measured in a 2θ-θ scan, a small tensile strain of ~0.35% has been determined for the optimal Nb film on (100)GaAs, whereas no strain has been found within the limits of probable error (~0.1%) for Mo on $(\bar{1}\bar{1}\bar{1})$GaAs.

IV. DISCUSSION

A substantial body of evidence suggests that the key variable which governs the microstructure of deposited films is the ratio of the substrate temperature T_s relative to the melting point of the deposit T_m, i.e., the "homologous" temperature T_s/T_m (Ref. 16). It has been found that the grain structure of deposited films depends systematically on the temperature of the substrate.[17,18] However, the systematic work of Grovenor, Hentzell, and Smith[14] showed that the final grain structure was the result of grain coarsening dur-

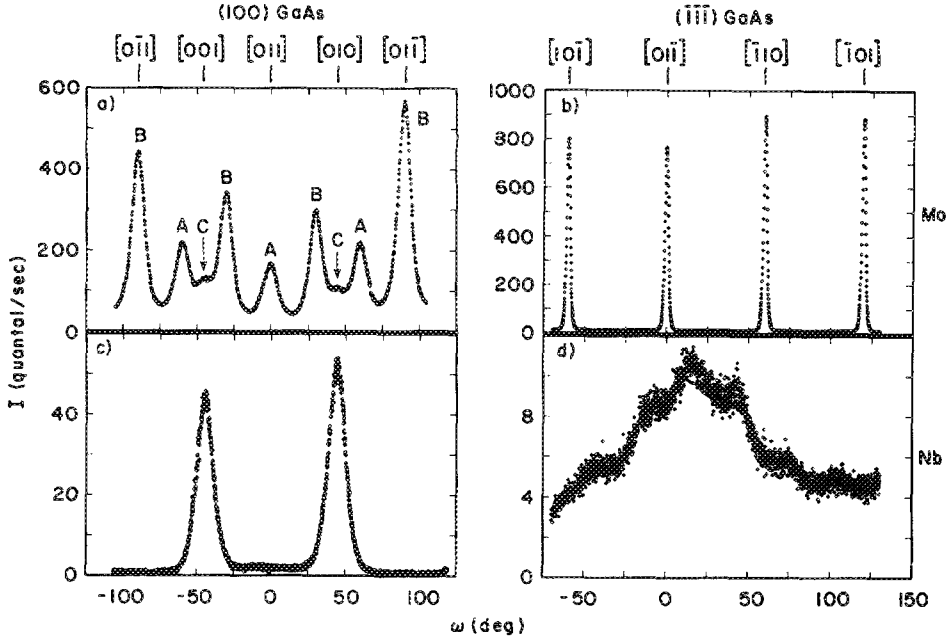

FIG. 6. GID ω scan of the (011) reflection of (a) Mo deposited on (100)GaAs; (b) Mo deposited on $(\bar{1}\bar{1}\bar{1})$GaAs; (c) Nb deposited on (100)GaAs; (d) Nb deposited on $(\bar{1}\bar{1}\bar{1})$GaAs. GaAs directions parallel to the interface are indicated at the top.

ing film thickening. Consequently, contrary to the conclusions of earlier investigators, at all substrate temperatures exceeding the threshold for grain-boundary mobility ($\sim 0.3\ T_m$), a single process, grain-boundary migration, was the key to the final grain morphology. At substrate temperatures $T_s \lesssim 0.3\ T_m$, the nature of the crystallization process remained obscure; it was, however, conjectured that condensation gave an unstable precursor phase which crystallized subsequently. It should be noted that the chemical potentials that drive grain growth in thin films are exceptionally large in comparison with their counterparts in bulk materials. Because of the small dimensions of the grains in the films and the limited thickness, the capillarity and the surface energy terms can both exceed typical values of the driving force in bulk recrystallization. In addition, compressive stresses can provide a driving force favoring grain growth and the supersaturation of defects can enhance the mobility of grain boundaries in thin films. Thus, for example, grain growth occurs in thin films of group Ib metals, such as gold or silver, at room temperature during vapor deposition and wet chemical deposition, while recrystallization of corresponding bulk material begins typically at about $0.4\ T_m$ and grain growth occurs at about $0.5\ T_m$.

It is well known that in the absence of any strong orienting effects of the substrate, the growth textures of fcc and bcc metals are fiber textures with fiber axes [111] and [110], respectively. The well-known phenomenon of the so-called epitaxial temperature, below which a polycrystalline film is formed and above which a single-crystal film results,[19] further indicates the key role of grain-boundary migration during film growth. This migration is eliminating boundaries between misaligned pairs of islands. Nucleation and grain-boundary migration are two of the key mechanisms by which film orientations are established. Oriented nucleation is the major factor leading to epitaxy for strongly interacting systems which grow layer by layer or in the Stranski–Krastanov mode; for Volmer–Weber systems, orientation is a postnucleation phenomenon involving topographic interactions with mobile islands and defects such as surface steps.[20,21] For strongly interacting systems, the substrate-deposit interfacial energy is a key factor and was the basis of an early concept that small misfit is a prerequisite for epitaxy. Neglecting chemical terms, low misfit is a criterion for low-energy substrate-deposit interfaces; however, following van der Merwe,[22] it is clear that relaxation, specifically formation of misfit dislocations, can substantially reduce the energy of an interface. Consequently, it is not unexpected that minimization of misfit, accommodated as misfit dislocations rather than elastically, proves to be a good guide to the various preferred orientations observed in bcc/fcc bilayers.[23]

In our work, the well-ordered structures obtained are usually characteristic for growth at substrate temperatures higher than those actually used by us. On the homologous scale, the best observed growth temperatures for Mo and Nb, 375 and 170 °C, were 0.22 and 0.16 T_m, respectively, much lower than the required threshold for grain-boundary mobility ($\sim 0.3\ T_m$). The grain size of the deposits, Fig. 4, also far exceeded the grain size expected from the zone model,[14] ~ 200 Å for the homologous temperatures used. However, when Mo was deposited onto $(\bar{1}\bar{1}\bar{1})$GaAs at $T_s = 375$ °C at a rate of 10 Å/s and a pressure of $\sim 5 \times 10^{-7}$ Torr, the expected 200 Å fine-grain randomly oriented polycrystalline deposit was obtained, as seen in Fig. 7. The implication is that under extremely clean conditions and low deposition rates, surface mobilities and grain-boundary mobilities are enhanced. It is noteworthy that tungsten, chemically a more refractory metal and structurally similar to molybdenum, grows as a random polycrystalline deposit under conditions where Mo shows a preferred orientation.[8]

The variation of the epitaxial quality with temperature of deposition, and in particular, the difference between the two metals studied, is also very interesting. For Mo, better epitaxy is obtained as T_s increases (up to 375 °C; higher T_s were not used to avoid compound formation), as expected from the above discussion. For Nb, the deterioration of epitaxy as the temperature increases above 170 °C is unexpected. We believe that this behavior can be attributed to a reaction that may take place at the interface between Nb and GaAs, possibly involving only a few monolayers. Recall that extensive formation of the compound NbAs after postdeposition annealing at 400 °C was observed (Fig. 5). This reaction might take place at lower temperatures only at the interface, to an extent sufficient to disturb the registry of the deposit with the substrate.

In no case was the surface-energy driven (110) texture observed. However, the known compounds of Mo or Nb with Ga or As together with the RHEED evidence that GaAs is covered by a monolayer of deposit (i.e., not island growth) all indicate that there is a strong interaction between deposit and substrate so that substrate effects are expected to be dominant. The orientation of Nb on (100) GaAs: (100)Nb‖(100)GaAs and [001]Nb‖[011]GaAs is known as the Baker–Nutting (BN) relationship.[23,24] The lattice mismatch between deposit and substrate, calculated from the bulk lattice parameters and verified by the diffraction pattern of Fig. 3(c), has the large value of -17%, causing the film to be under tension in the absence of relaxation. Presumably most of this misfit is relaxed by misfit dislocations. We note that an in-plane rotation of the Nb mesh by 45° will result in the so-called BN45 epitaxy.[23] This orientation has about the same lattice mismatch, but with opposite sign, resulting in film compression. Such an epitaxy has not been found in this study. It may be argued that, due to the anharmonic shape of the interatomic potential, film tension is energetically favored over film compression for the same amount of strain. This argument applies to the nucleation stage of the deposition, before the stress relaxation by misfit dislocations has occurred. As reported by Grovenor, Sutton, and Smith,[23] BN epitaxy is prevalent for a bcc deposit on a fcc substrate with a lattice parameter ratio of $r < 0.78$, while BN45 epitaxy can be obtained only for $r > 0.92$. This behavior was attributed to a tendency to minimize the elastic strain energy. For Nb/(100)GaAs, with a lattice parameter ratio of $r = 0.585$, r is beyond the range considered by Grovenor, Sutton, and Smith.[23] While it might be expected that the BN orientation would be preferred for a range of values of r less than 0.707, which is the value for zero misfit, the limit of the

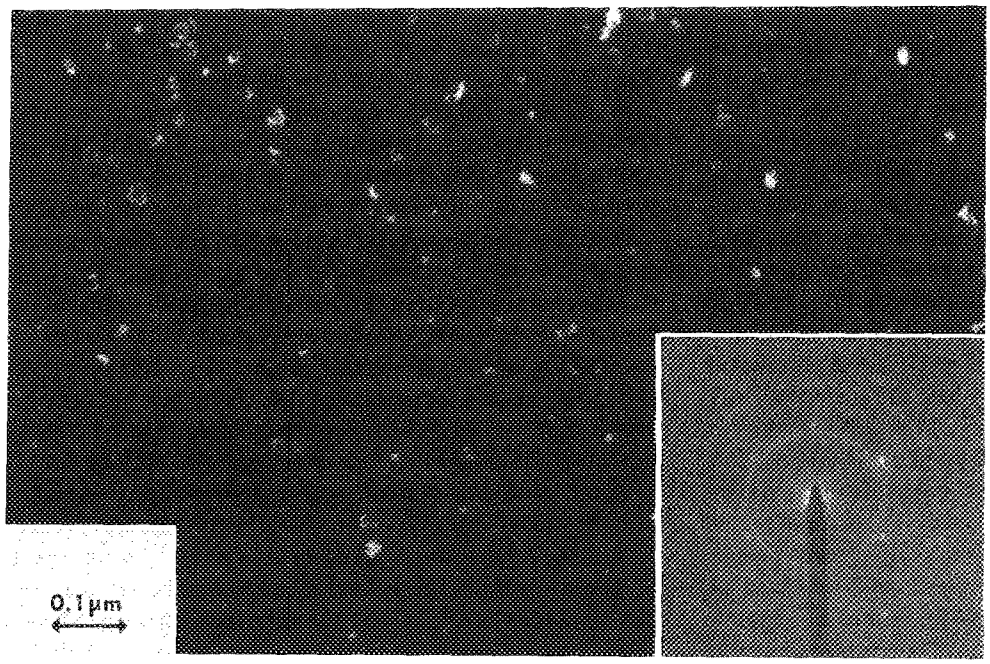

FIG. 7. Transmission electron diffraction pattern (a) and Mo (100) dark-field image (b) of a molybdenum film deposited on $(\bar{1}\bar{1}\bar{1})$GaAs under conventional conditions: $p \sim 5 \times 10^{-7}$ Torr, rate ~ 10 Å/s.

stability has not been addressed at all until now. It was found that Nb grows also with a (100) texture on $(\bar{1}\bar{1}\bar{1})$GaAs substrate; however, as mentioned above, the azimuthal misalignment with respect to the GaAs substrate is presently not understood.

It should be noted that the BN45 epitaxy has been reported for bcc Fe on (100)GaAs with a lattice parameter ratio of $r = 0.507$ (Ref. 5). For this orientation, the lattice mismatch between a lattice with twice the lattice parameter of iron and that of GaAs amounts to 1.4%, causing the film to be under compression in the absence of relaxation.

Mo shows a preference for the (111) texture on both (100) and $(\bar{1}\bar{1}\bar{1})$GaAs. Its alignment on the $(\bar{1}\bar{1}\bar{1})$ plane is much better than on the (100) plane, evidenced by the (110)Mo spots in Fig. 3(b) as compared to the arcs in Fig. 3(a), and also by the GID results in Figs. 6(a) and 6(b). The calculated lattice mismatch on the $(\bar{1}\bar{1}\bar{1})$ substrate is 11%, causing the film to be under compression in the absence of relaxation. On the (100)GaAs substrate, the epitaxial relationship found was (111)Mo$\|$(100)GaAs with $[01\bar{1}]$Mo$\|[01\bar{1}]$GaAs. The smallest nearest neighbor linear misfit is $+11\%$, whereas the second neighbor misfit in the perpendicular direction, along [011]GaAs, is -3.5%. It should be emphasized that the x-ray data show that the strain in the films is smaller than the large mismatch would indicate, implying that extensive relaxation has occurred. Misfit dislocations with a spacing b/ϵ (b is Burger's vector, and ϵ the calculated misfit) are required in a partially coherent interface, but would be too close to be resolved in this work. It is noteworthy that the GID study of Mo/(100)GaAs revealed that, beside the strong signals from (111) oriented Mo domains, an extremely weak BN epitaxy component was also present [see Fig. 6(a)], suggesting that the lower value of the lattice parameter ratio for the system, $r = 0.557$, might be at the transition to still another regime, not considered by Grovenor's rule.[23]

Symmetry considerations suggest that variants of the orientation relationships given above will occur, and in certain cases the diffraction patterns reveal multiple positioning. For example, in Fig. 3(a), 110 maxima from all four {111} variants of the Mo deposit on (100)GaAs can be recognized. In contrast, the {111} diffraction pattern in Fig. 3(b) conceals the fact that two (111)Mo patterns are superimposed. (In fact, similar double positioning has also occurred in the $(\bar{1}\bar{1}\bar{1})$GaAs buffer layer.) This double positioning would be a major difficulty if the growth of a top layer of GaAs for device applications were attempted. In fact, none of the deposits, with the possible exception of Mo on $(\bar{1}\bar{1}\bar{1})$GaAs, had a perfection that warranted investigation of the quality of a second GaAs epilayer.

Finally, the evidence from RHEED on the delayed crystallization shows that the nucleation of oriented crystalline Mo and Nb occurs only when the deposit thickness exceeds ~ 30 Å. This observation may be explained in two ways: (1) there is an incubation time or critical thickness for crystallization; (2) an intermediate interfacial compound layer forms and acts as a template for subsequent growth of Mo or Nb, as known for Au on GaAs.[4] Interrupting the metal deposition and maintaining T_s for up to 1 h at thickness of less than 30 Å did not result in crystallization, rendering unlikely the hypothesis of incubation time. Regarding the second possibility, *in situ* Auger spectroscopy indicated that Ga and As are mobile during deposition (small amounts were detected on the surface), and it was shown that postdeposition heating can give epitaxial compounds with Nb (see Fig. 5). However, no compounds were detected in as-deposited films. Therefore, the presence of the intermediate compound layer was not proven either. Given this knowledge, a defini-

tive conclusion concerning the origin for the delayed crystallization cannot be reached.

V. SUMMARY

We have found that molybdenum has a strong preference to grow epitaxially with a (111) orientation on $(\bar{1}\bar{1}\bar{1})$ and (100) GaAs despite a large misfit. Niobium, on the other hand, grows with a (100) texture on both substrates. For both metals, the orientational spread is smallest when the lattice planes parallel to the interface have the same symmetry in film and substrate. The best epitaxial Mo films on $(\bar{1}\bar{1}\bar{1})$ GaAs were obtained when grown at a substrate temperature $T_s \sim 375$ °C. On the other hand, in the case of Nb on (100) GaAs, the quality was best for a substrate temperature $T_s \sim 170$ °C. As the temperature was increased or decreased, the ratio of aligned to nonaligned grains gradually decreased.

Our results indicate that the zone model for film structure needs to be modified for deposition under ultrahigh vacuum conditions because of enhanced surface and grain-boundary mobility. In addition, it has been found that Mo and Nb crystallization is a postcondensation phenomenon, possibly because of interface compound formation or the existence of a thickness dependent metastable precursor phase.

Note added in proof: The evidence for grain sizes up to several hundred nanometers in the TEM micrographs of Fig. 4 seems to be at variance with the grain sizes $\lesssim 200$ Å measured by GID. We would like to point out that the "grain" size measured by x-ray diffraction is really the size of coherently scattering domains that is determined by small-angle boundaries, dislocations, and other crystal structure faults, and that can be much smaller than the grain size measured by TEM.

[1] See, for example, *Metal-Semiconductor Schottky-Barrier Junctions and their Applications*, edited by B. L. Sharma (Plenum, New York, 1984).
[2] D. V. Geppert, Proc. Inst. Radio Eng. **50**, 1527 (1962); D. Khang, *ibid.* 1534 (1962).
[3] G. Landgren, R. Ludeke, and C. Serrano, J. Cryst. Growth **60**, 393 (1982).
[4] T. Yoshiie, C. L. Bauer, and A. G. Milnes, Thin Solid Films **111**, 149 (1984).
[5] J. R. Waldrop and R. W. Grant, Appl. Phys. Lett. **34**, 630 (1979).
[6] G. A. Prinz and J. J. Krebs, Appl. Phys. Lett. **39**, 397 (1981).
[7] G. A. Prinz, Phys. Rev. Lett. **54**, 1051 (1985).
[8] J. Bloch, M. Heiblum, and Y. Komem, Appl. Phys. Lett. **46**, 1092 (1985).
[9] A. Segmüller, Adv. X-Ray Anal. **29**, 353 (1986).
[10] M. Eizenberg, D. A. Smith, M. Heiblum, and A. Segmüller, Appl. Phys. Lett. **49**, 422 (1986).
[11] M. Heiblum, J. Bloch, and J. J. O'Sullivan, J. Vac. Sci. Technol. A **3**, 1885 (1985).
[12] W. C. Marra, P. Eisenberger, and A. Y. Cho, Appl. Phys. Lett. **50**, 6927 (1979).
[13] See, for example, C. S. Barrett, and T. B. Massalski, *Structure of Metals* (McGraw-Hill, New York, 1966).
[14] C. R. M. Grovenor, H. T. G. Hentzell, and D. A. Smith, Acta Metal. **32**, 773 (1984).
[15] *Powder Diffraction File* (JCPDS-International Centre for Diffraction Data, Swarthmore, PA), Card No. 17-896.
[16] See, for example, C. A. Neugebauer, in *Handbook of Thin Film Technology*, edited by L. I. Maissel and R. Glang (McGraw-Hill, New York, 1970), p. 8-3.
[17] B. A. Movchan and A. V. Demchishin, Fiz. Metal. Metalloved. **28**, 653 (1969).
[18] J. A. Thornton, Ann. Rev. Mater. Sci. **7**, 7 (1977).
[19] See, for example, I. H. Khan, in *Handbook of Thin Film Technology*, edited by L. I. Maissel and R. Glang (McGraw-Hill, New York, 1970), p. 10-1.
[20] D. A. Smith and M. M. J. Treacy, Appl. Surf. Sci. **11/12**, 131 (1982).
[21] D. A. Smith, J. T. Wetzel, and A. R. Taranko, Mater. Res. Soc. Symp. Proc. **37**, 77 (1985).
[22] J. H. van der Merwe, Proc. Phys. Soc. London A **63**, 616 (1950).
[23] C. R. M. Grovenor, A. P. Sutton, and D. A. Smith, Scr. Metal. **18**, 939 (1984).
[24] R. G. Baker and J. Nutting, *Precipitation Processes in Steel*, Special Report No. 64 (Iron and Steel Institute, London, 1959), p. 1.